ACS OMEGA

Open Access

This article is licensed under CC-BY-NC-ND 4.0

http://pubs.acs.org/journal/acsodf

Article

# Mechanically Robust Poly(vinyl alcohol)–Egg White Composite Hydrogel with Enhancing Biocompatibility by Unidirectional Nanopore Dehydration

Ji-Xin Li* and Yu-Qing Zhang*

Cite This: *ACS Omega* 2023, 8, 33763–33773

Read Online

ACCESS | Metrics & More | Article Recommendations

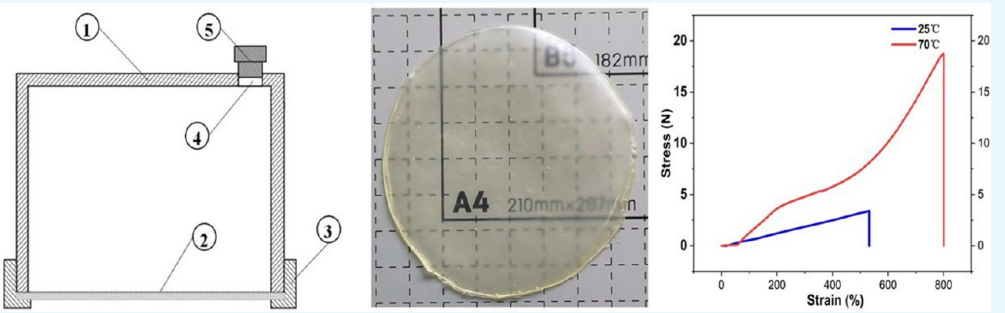


**ABSTRACT:** A simple and green method, unidirectional nanopore dehydration (UND), directly processes 10% poly(vinyl alcohol) (PVA) aqueous solution containing 20% egg white (EW) into a composite hydrogel membrane (PVA–EW). The tensile strength and elongation of the UND-based PVA–EW at 25 °C were 0.91 MPa and 534.17%, respectively, while the two values at 70 °C were increased by 700 and 38%, respectively. The PVA–EW (70 °C) was still dominated by random coils and $\alpha$-helical structures. The hydroxyl groups of intramolecules and intermolecules of both PVA and EW could be able to combine and form either more hydrogen bonds or stronger hydrogen bonds. PVA–EW is soft and translucent, has good mechanical properties, and has a porous networked structure with pores that have a diameter of 1–10 $\mu$m. L-929 mouse fibroblasts were found to be able to adhere, grow, and proliferate well on the hydrogel composite membrane. This novel PVA–EW biomaterial has potential applications in biomaterials especially medical tissue engineering.

## 1. INTRODUCTION

Poly(vinyl alcohol) (PVA) is a biodegradable synthetic polymer material prepared from polyvinyl acetate via hydrolysis. Its side chains contain many hydrophilic hydroxyls (−OH) groups. PVA-based polymer materials have good mechanical, chemical, and physical properties; are nontoxic; have barrier-like properties; are resistant to chemicals; and have film-forming capabilities. It is widely used in the field of biomaterials in applications such as wound care, nanomaterials, packaging materials, biofilm separation, immobilized carriers, etc.[1−4] Most PVA-based composite hydrogels are prepared by chemical cross-linking methods.[5−7] PVA–boronate hydrogel prepared by boronate esterification was used as a fluorescent chemical sensor for copper ion in water.[8] Ali et al. described that the glucose-responsive protein–PVA hydrogels prepared by using formylphenylboronic acid-based cross-linkers have great potential as smart insulin release for in vivo applications.[9,10] A physical preparation method is mainly based on cyclic freeze–thawing methods,[11] and there have also been studies focusing on physical cross-linking methods such as irradiation, heat treatment, and acetone desolvation.[12−14] However, PVA materials can still be improved in terms of their resistance to water, processability, and flexibility. Therefore, PVA materials are usually modified by blending with other polymer materials, such as adding artificial or natural polymers, polysaccharides, inorganic salts, or other inorganic substances.[15−17] PVA biomaterials, especially PVA composite hydrogels, are often combined with natural polymers such as silk fibroin, soy protein isolate, casein, and other proteins.[18−20] Among these additives, PVA composite films that are prepared by the addition of the plasticizer casein using the simplest casting method can be biodegradable and are mainly used for food packaging materials, wound dressing materials, and enzyme carriers.[21−23] The most commonly used method to produce porous composite hydrogels or hydrogel films from PVA and other proteins is cyclic

Received: June 12, 2023
Accepted: August 30, 2023
Published: September 6, 2023

© 2023 The Authors. Published by American Chemical Society

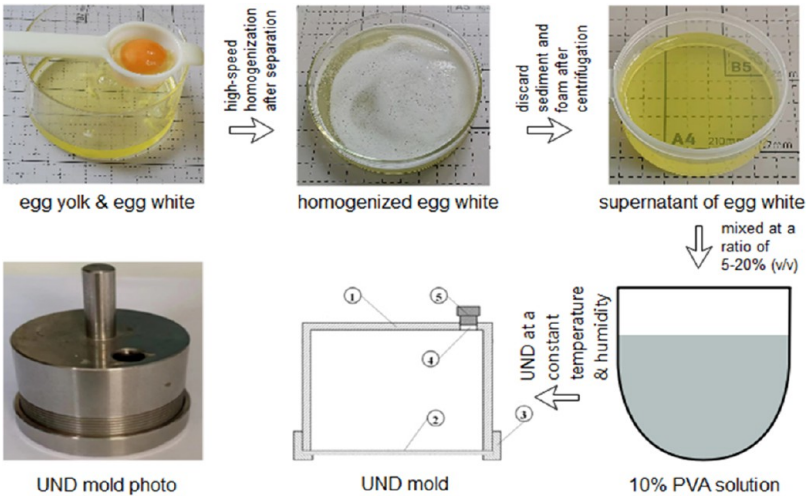


**Figure 1.** Schematic for the process of PVA−EW hydrogel composition membrane preparation UND mold: ① film-forming cup body, ② filter film with nanopore, ③ fixed flange, ④ sampling hole, and ⑤ rubber plug.

freeze−thaw, but the pore size of hydrogel membranes prepared by the cyclic freeze−thaw method is too large to be controlled, which limits their applications.

Egg white (EW) is a cheap and abundant natural source of important proteins such as ovalbumin and lysozyme. Due to its antibacterial properties and biodegradability, it is an ancient biological material. EW is mainly composed of 54% ovalbumin, 12% ovotransferrin, 11% ovomucoid, 3.5% ovomucin, and 3.5% lysozyme. Due to its unique thermal gelling properties, it has been used in many new applications[24−26] in the field of biomaterials, such as in the form of hydrogels, food packaging, biosensors, drug slow release, nanomaterials, etc. However, these EW or EW-based biomaterials have poor mechanical properties, and cross-linking agents are often added to make wound dressings and composite films.[27,28] By mixing EW into PVA and other solutions, the cyclic freeze−thawing method can be used to make PVA−EW bionanocomposite hydrogels, composite scaffolds, smart colorimetric membrane, and other materials.[29−31] A mixed solution of PVA and EW could be electrospun to make a composite fiber wound dressing.[32,33] However, there have been few studies on the use of PVA and EW in biomaterials to make composite hydrogel membranes or scaffolds by green physical methods, especially in the context of materials used in medical tissue engineering.

In this article, we will use our team's newly developed unidirectional dehydration technology (UND),[34] where one-way downward dehydration is achieved by using a nanopore semi-permeable cellulose membrane, to make a PVA−EW composite hydrogel with green, strong mechanical properties and excellent biocompatibility. We will also conduct a detailed investigation into its physical, chemical, mechanical, and structural properties, as well as its biocompatibility.

## 2. MATERIALS AND METHODS

**2.1. Experimental Materials.** PVA (PVA-124, viscosity: 54−66 mPa·s) was purchased from China Aladdin Co., Ltd. Hen eggs (Lanfei brand) were purchased from Shanghai Dahe Egg Products Co., Ltd. (China).

**2.2. PVA Aqueous Solution Preparation.** 10% PVA aqueous solution was prepared according to the method reported recently by authors.[35]

**2.3. PVA−EW Hydrogel Composite Membrane Preparation.** The separation of EW from a hen egg and the preparation of homogenized EW solution from thin and thick EWs were carried out according to the method recently reported by the authors.[36] The homogeneous EW solution was mixed with 10% PVA solution at a ratio of 5:20% (v/v). 5 mL of this mixed sample solution was added to a mold that was composed of a dialysis membrane with a molecular weight cutoff of 10 kDa as described at the bottom of the box.[32] The mold was placed horizontally at room temperature or in a chamber held at a constant temperature and humidity and subjected to unidirectional dehydration (UND) through a nanopore for 15−20 h (Figure 1). After the film was formed, the mold was opened and the PVA−EW composite hydrogel was removed. The film was stored at 4 °C for later use.

**2.4. Mechanical Properties Analysis.** After immersing in water at 37 °C for 24 h, the tensile test of the PVA−EW hydrogel film (5.0 mm × 30 mm × 0.8 mm) was carried out using an INSTRON 3365 universal material testing machine according to the method recently reported by the authors.[32] Five measurements were repeated per group.

**2.5. Infrared, X-Diffraction, and Thermal Performance Measurement.** A dry sample of the hydrogel film was ground into a fine powder. 5.0−20 mg of powdered sample was used for detection on a Nicolet 6700 infrared spectrometer (Thermo Fisher), for the measurement of X-ray diffraction pattern using an X'pert Pro MPD X-ray diffractometer (PANalytical, Holland Panalytical), and for the analysis of thermogravimetry (TG), derivative TG (DTG), and differential scanning calorimetry (DSC) curves using an SDT2960 differential thermoregeneration instrument (30−1400 °C; TA Instruments) according to the method recently reported by the authors.[32] The hydrogel film was cut to a certain size and tested by the small-angle X-ray scattering SAXS (Anton Paar SAXSess MC2, Austria).

**2.6. SEM Observation.** After immersing in liquid nitrogen for a few minutes, the resulting cracked sample was fixed onto the sampling stage and sprayed with gold for 60 s. Then, the surface of the sample and the apparent shape of the cross section were observed using a Hitachi S-4700 cold field emission scanning electron microscope (SEM, Hitachi Co., Ltd., Japan).

**2.7. In Vitro Enzymolysis.** According to the method reported by Li et al. with slight modification,[37] the enzymes



https://doi.org/10.1021/acsomega.3c04171
ACS Omega 2023, 8, 33763−33773

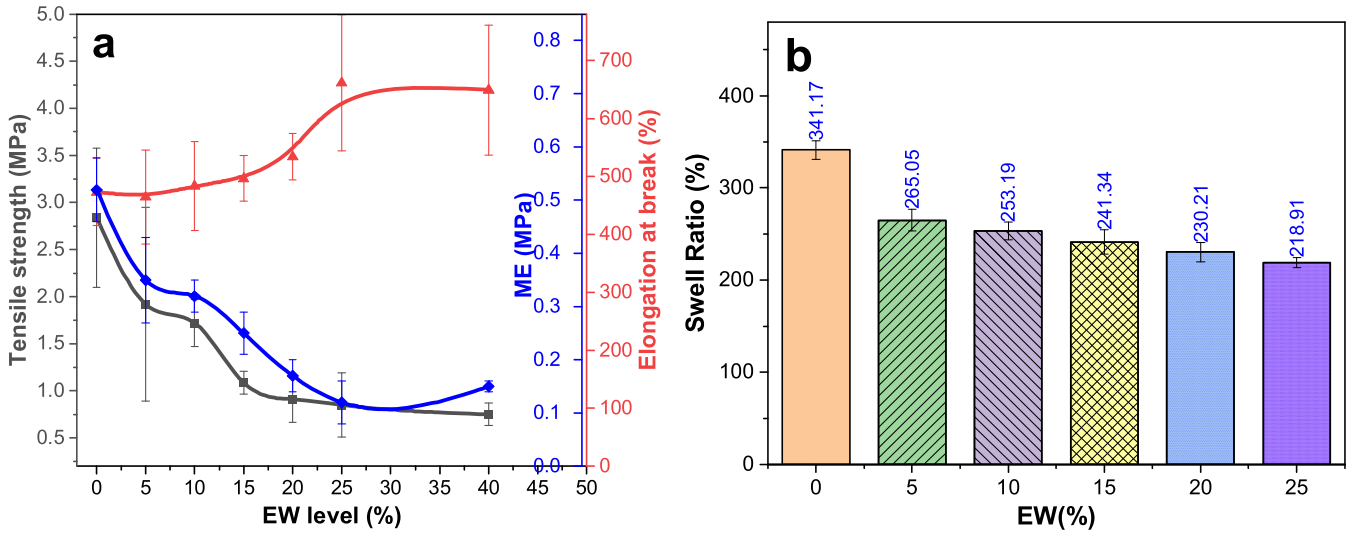


**Figure 2.** Effect of EW level on mechanical properties (a) and swelling ratios (b) of PVA−EW hydrogel films; the film size when stretched is 5 mm × 30 mm × 0.8 mm.

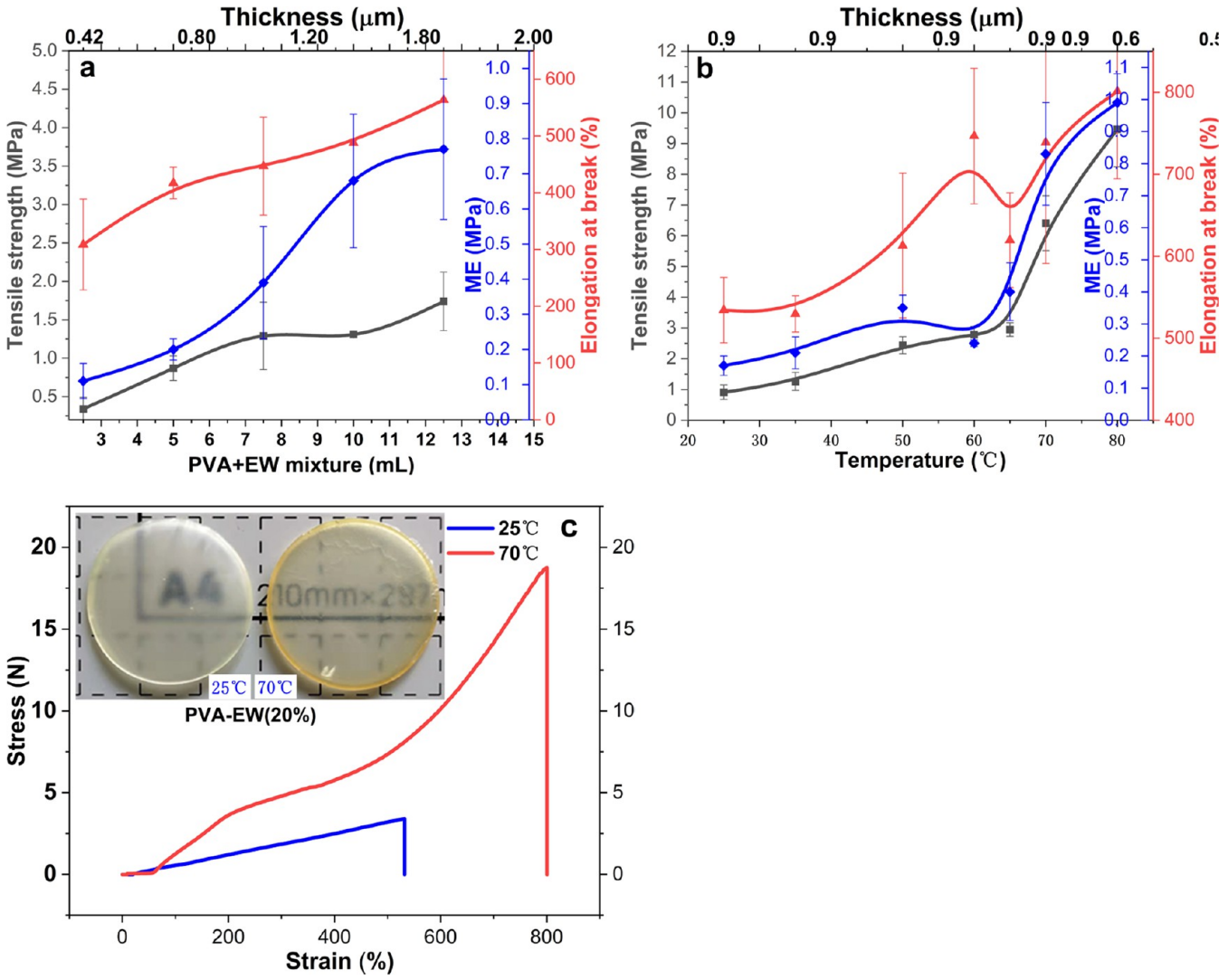


**Figure 3.** Effects of film thicknesses (a) and UND temperatures (b) on mechanical properties of PVA−EW and appearance and stress−strain curves (c) of PVA−EW (20%) prepared at 25 and 70 °C.



https://doi.org/10.1021/acsomega.3c04171
ACS Omega 2023, 8, 33763−33773

trypsin and alkaline protease were prepared into 140 U/mL enzyme stock solution with phosphate-buffered saline (PBS). The two enzymes were trypsin (pH 7.4−7.6, 37 °C) and alkaline protease (pH 9.0−12.0, 40−50 °C). The prepared enzyme solution was filtered and sterilized. These aseptic enzyme solutions were diluted 10 times with PBS before use. Around 0.15 g of the dry PVA−EW hydrogel was immersed in ∼5 mL of enzyme solution; this process was repeated for three samples in each group in a 12-well plate. The sample immersed in the trypsin solution was placed in a shaker (110 rpm), while the sample immersed in the alkaline protease solution was placed in a shaker held at a constant 50 °C for degradation (110 rpm). The degradation was observed and the enzyme solution was replaced daily. Every 2 days, the samples were taken out, washed with PBS, dried, and weighed.

**2.8. Cell Culture.** The method reported by Wang et al. was slightly improved,[38] and the cytocompatibility was tested on mouse L-929. A round sample of the hydrogel membrane with a diameter of 10 mm was prepared and cultured in a 48-well plate. During the culture period, the 48-well plate was removed from the incubator daily; the cell growth was observed using an inverted fluorescence microscope and recorded. CCK-8 was used to determine cell viability.

**2.9. Statistics.** The data obtained in the experiment were processed using the Origin 10 software. The results are presented in the form of a mean ± standard error.

## 3. RESULTS

**3.1. Effect of EW Incorporation on Mechanical Properties and Swelling Rates.** To understand the influence that the addition of EW has on the mechanical properties of the PVA hydrogel composite membrane, EW was added to the aqueous PVA solution at volumes of 5, 10, 15, 20, 25, and 40% (v/v), and was dehydrated unidirectionally via film nanopores at room temperature for 24 h to form a translucent PVA−EW composite hydrogel film. Figure 2a presents the results of the mechanical performance tests on PVA−EW hydrogels with different proportions of EW. It can be seen that as the EW content increases, the tensile force ($F_{max}$) and tensile strength ($\sigma$) of the film gradually decreases; the $\sigma$-value started at 2.84 MPa when the hydrogel contained no EW, and in the sample with 40% EW, the $\sigma$-value was only 0.75 MPa. Similarly, the elastic modulus (ME) of the sample decreases from 0.52 to 0.15 MPa. However, the film's elongation at break (EB) increased as the amount of EW was increased, exhibiting a dose−effect relationship; the elongation was 473.20% when no EW was added and increased to 649.02% at 40% EW. These results indicate that the addition of EW significantly reduces the tensile strength and elastic modulus of the PVA−EW composite hydrogel film, while the elongation at break increases significantly following a dose−effect relationship. However, when the EW reaches 40%, the elongation at break no longer increases. In addition, when the hydrogel film is composed of more than 40% EW, a small amount of EW protein will separate from the film when it is soaked in water. Therefore, a hydrogel composite film containing 20% EW, henceforth referred to as PVA−EW (20%), was used in the following experiments.

The influence of EW content on the swelling exhibited by the PVA−EW composite hydrogel films is shown in Figure 2b. The swelling ratio of the pure PVA hydrogel film reached 341.17%; after the addition of 5% EW, the swelling ratio of the hydrogel composite film decreased significantly to 265.05%. As the amount of EW added was increased, its swelling ratios continued to decrease significantly. For every 5% increase in EW, the swelling ratio drops by an average of 11.5%. However, when 25% EW was added, the swelling ratio of the composite hydrogel film decreased to 218.9%. This suggests that the amount of EW added can adjust not only the tensile strength of the composite hydrogel but also its elongation at break.

**3.2. Hydrogel Composite Film Thickness.** For this experiment, five different volumes of PVA−EW mixtures were used to create PVA−EW (20%) composite hydrogel membranes with different thicknesses. Their mechanical properties are presented in Figure 3a. The results show that larger volumes resulted in greater thicknesses in the formed films. In addition, as the thickness of the film increased, the tensile force, tensile strength, elongation at break, and compression modulus also increased. The results exhibited a dose−effect relationship. When a maximum volume of 12.5 mL was used, the maximum tensile force was 17.32 N, the tensile strength reached 1.74 MPa, the elongation at break was 563.53%, and the compressive modulus was 0.77 MPa.

**3.3. Temperature Effects.** To explore the influence of environmental factors on the formation of composite hydrogel membranes using UND, we prepared these composite membranes at seven different temperatures. This was accomplished by placing the mold containing the mixed PVA−EW solution into a box that was held at a constant temperature and humidity. The temperature was changed to the desired experimental values when the relative humidity was at a constant 50% (Figure 3b). At 25 °C, the maximum tensile force of the sample was 3.64 N and its elongation at break was 534.17%. When the temperature was increased during UND, the mechanical strength and elongation at break increased and the compression modulus also increased, but the thickness of the hydrogel film decreased. At a processing temperature of 80 °C, the mechanical strength of the sample was 9.46 MPa and its elongation at break was 801.16%. Here, it should be noted that a small peak in elongation at break at 60 °C in Figure 3b may be caused by temperature control errors. At processing temperatures higher than 80 °C, a small amount of white EW protein precipitated into the formed hydrogel film. Therefore, in the following experiments, the PVA−EW hydrogel composite films were generally prepared at two temperatures: 25 and 70 °C.

**3.4. Stress−Strain Curves.** The stress−strain curves of the hydrogel membranes prepared at a constant temperature of 25 and 70 °C at 50% relative humidity (RH) are presented in Figure 3c. At a processing temperature of 25 °C, the PVA−EW film is semitransparent (Figure 3 inset, left photograph). Its maximum tensile force was 3.41 N, its elongation at break was 532.03%, and its tensile strength was 0.85 MPa. At a processing temperature of 70 °C, the PVA−EW film is semitransparent with a light yellow coloration (Figure 3 inset, right photograph). The maximum tensile force of the hydrogel composite membrane was as high as 18.76 N, its elongation at break was 800.71%, and its tensile strength was 6.25 MPa. It can be seen that as the temperature of UND was increased from 25 to 70 °C, the 20% EW protein contained within the film did not denature, the tensile strength of the hydrogel composite film increased by more than seven times, and its elongation at break increased by 50%. The results from Figure 3b,c thus indicate that the temperature of UND has a strong influence on the mechanical properties of the resultant PVA−EW hydrogel; in other words, we can effectively control the properties of the composite hydrogel through temperature regulation. When the hydrogel film was prepared at 70 °C, the increase of temperature led to the


https://doi.org/10.1021/acsomega.3c04171
ACS Omega 2023, 8, 33763−33773

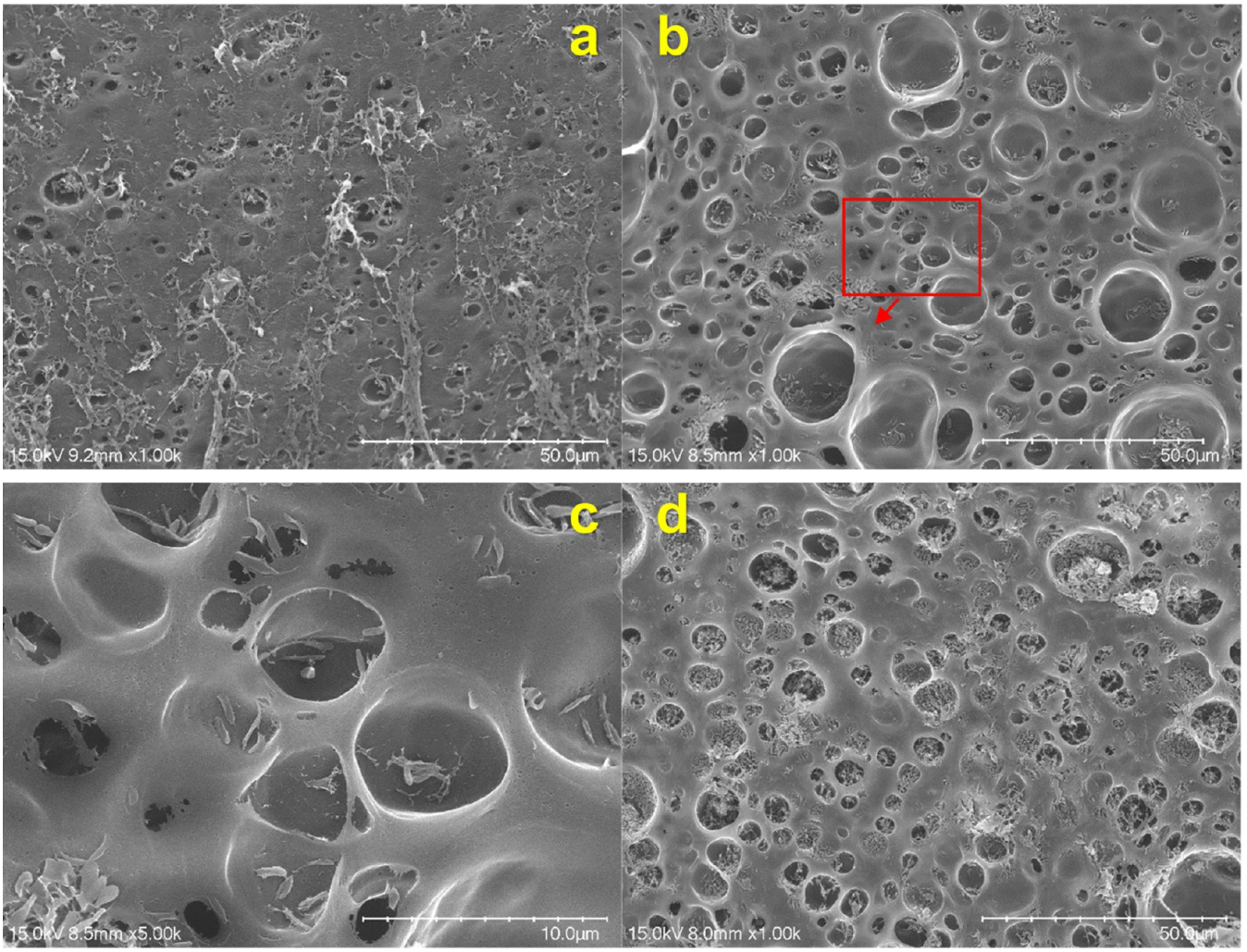


**Figure 4.** Cross-sectional photographs of PVA−EW hydrogel composite membranes. PVA−EW (5%) hydrogel film containing 5% EW (1000×) at 25 °C (a), PVA−EW (20%) hydrogel film containing 20% EW (1000× and 5000×) at 25 °C (b, c), and PVA−EW (20%) hydrogel film containing 20% EW (1000×) at 70 °C (d).

**Table 1. Effects of EW Addition and Temperature on the Porosity of PVA−EW Hydrogel Membranes**

| PVA hydrogels | mean size (μm) | ±SD | max | mini | pore number | ±SD | porosity (%) | ±SD |
|---|---|---|---|---|---|---|---|---|
| PVA−EW (5%) 25 °C | 2.6 | 2.0 | 9.0 | 0.2 | 210 | 5 | 14.2 | 1.5 |
| PVA−EW (20%) 25 °C | 8.9 | 6.7 | 25.3 | 0.6 | 260 | 8 | 52.0 | 3.1 |
| PVA−EW (20%) 70 °C | 6.0 | 3.9 | 18.7 | 0.5 | 215 | 6 | 31.0 | 1.4 |

acceleration of molecular motion, the shortening of film formation time, the formation of more and stronger hydrogen bonds between the hydroxyl groups of PVA and EW molecules, thus forming a denser structure with enhanced mechanical properties, and the thickness of the hydrogel film was thinner.

In addition, the PVA−EW hydrogel above formed by UND at 70 °C showed a pale yellow color (Figure 3 inset, right photograph), which is mainly caused by the Maillard reaction in the EW of PVA−EW hydrogel. The EW sample prepared in this experiment has not been sweetened, so the homogenized EW contains a certain amount of reducing sugar, such as glucose. The UND of PVA and EW mixed solution at a higher temperature leads to the Maillard reaction between reducing sugar and free amino acid residues in protein.[39,40]

**3.5. Microstructure Observations.** The structure of the fracture surface of the PVA−EW hydrogel membrane is shown in Figure 4. As the EW content increases, the wet PVA−EW hydrogel film becomes softer. When observed under an SEM magnification of 1000×, it was revealed that the fracture surface of the membrane formed at both 25 and 75 °C has a porous structure. At an EW content of 5%, the distribution of pore sizes ranges from 0.2 to 9.0 μm, with a mean value of 2.6 μm (Table 1 and Figure 4a). When the EW content was increased to 20% (Figure 4b,c), the pore sizes were found to be significantly larger, and the average pore size was observed to have increased by a factor of three. Additional careful observation revealed that there was one type of pore that was particularly large (∼25 μm), while the other type of pore was more numerous but exhibited smaller pore diameters (∼5 μm). In addition, the fracture surface was smoother. When the temperature of directional dehydration was increased to 70 °C, the average pore size decreased by ∼30%. Therefore, the size and distribution of pore may be mainly related to the EW level and temperature of nanopore dehydration during preparation. The size distribution of the



https://doi.org/10.1021/acsomega.3c04171
ACS Omega 2023, 8, 33763−33773

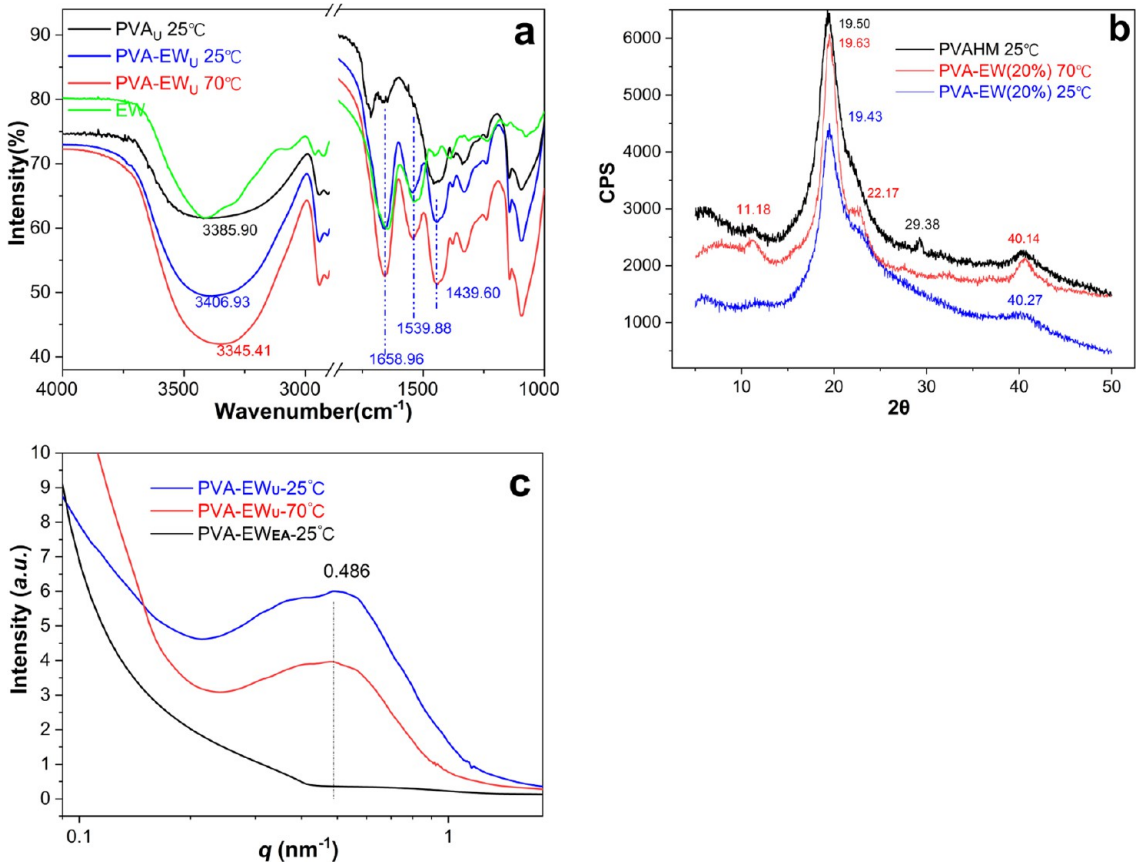


**Figure 5.** FTIR spectra (a), X-ray diffraction (b), and SAXS (c) patterns of PVA−EW hydrogel film containing 20% EW formed at 25 and 70 °C. PVAHM_25 °C is the UND-based PVA hydrogel film alone at 25 °C as a control group.

second type of pore was similar, but the fracture surface was relatively rough; in addition, a large number of small particles (less than 1 $\mu$m) also appeared. These may be due to the aggregation of a few EW protein molecules at higher temperatures (Figure 4d). These results show that PVA−EW (20%) hydrogel composite membranes can still form porous hydrogel structures, that the two materials are compatible, and that the pore size had significantly increased. Our observations suggest that the EW concentration can be used to adjust the pore size of the PVA−EW hydrogel composite membrane.

**3.6. FTIR Spectra.** Figure 5a shows the infrared spectra (FTIR-ATR) of a single PVA hydrogel film formed by UND at 25 °C and of two PVA−EW (20%) hydrogel composite films formed at 25 and 70 °C. The very broad peak at 3415.31 cm$^{-1}$ in the PVA hydrogel film alone (PVA 25 °C in Figure 5a) corresponds to the stretching vibrations of the −OH group. The peak at 1715.85 cm$^{-1}$ is characteristic of the −C═O stretching vibration, and the peak at 1456.75 cm$^{-1}$ represents the stretching vibration of the −CH group (black line). At 25 °C, the PVA−EW (20%) hydrogel composite membrane exhibited a peak at 1658.96 cm$^{-1}$ corresponding to the amide I band, while the peak of the amide II band was at 1539.88 cm$^{-1}$, corresponding to the $\alpha$-helical structure. In addition, the peak of the −OH groups belonging to the EW appeared at 3396.14 cm$^{-1}$, which can combine with the −OH groups from the PVA to form strong hydrogen bonds, which can improve the interactions between molecules, increase the cohesion of the biopolymer matrix, reduce its water sensitivity, and result in a peak at 1439.60 cm$^{-1}$ (blue line). When the hydrogel film was formed at 70 °C, the −C═O stretching peak from the amide I band and the −NH bending peak from the amide II band did not shift significantly. In contrast, the stretching vibration peak of the −OH group shifted significantly to 3345.41 cm$^{-1}$ (red line), which is due to the improved hydrogen bonding capability within the composite hydrogel at this UND temperature. The lack of changes to the amide I and amide II bands indicate that when the processing temperature was increased to 70 °C, the protein structure of the PVA−EW hydrogel membrane did not change significantly. However, the significant shift in the vibration peak of the −OH group indicates that there are more numerous and stronger hydrogen bonds within the composite hydrogel; this is consistent with its enhanced mechanical properties.

**3.7. XRD Patterns.** To study the change in the crystal structure of the PVA/EW blend, the X-ray diffraction (XRD) pattern of the samples was analyzed (Figure 5b). The PVA hydrogel film alone as a control exhibits strong peaks at 19.50 and 40.14° as well as weak peaks at 11.18 and 29.38°. The characteristics of the two main peaks of the PVA−EW (20%) hydrogel composite membrane did not change significantly, suggesting that there were no observable changes in the crystal structure due to the addition of EW proteins. However, the main peak of the composite membrane prepared at 70 °C was found to have shifted slightly to 19.63°, while the shifts in the three smaller peaks at 11.18, 22.17, and 40.14° were more significant. This indicates that faster one-way dehydration at higher temperatures can change the crystal structure of the hydrogel composite film. It is possible that the hydroxyl groups between adjacent segments formed stronger and more numerous


https://doi.org/10.1021/acsomega.3c04171
ACS Omega 2023, 8, 33763−33773

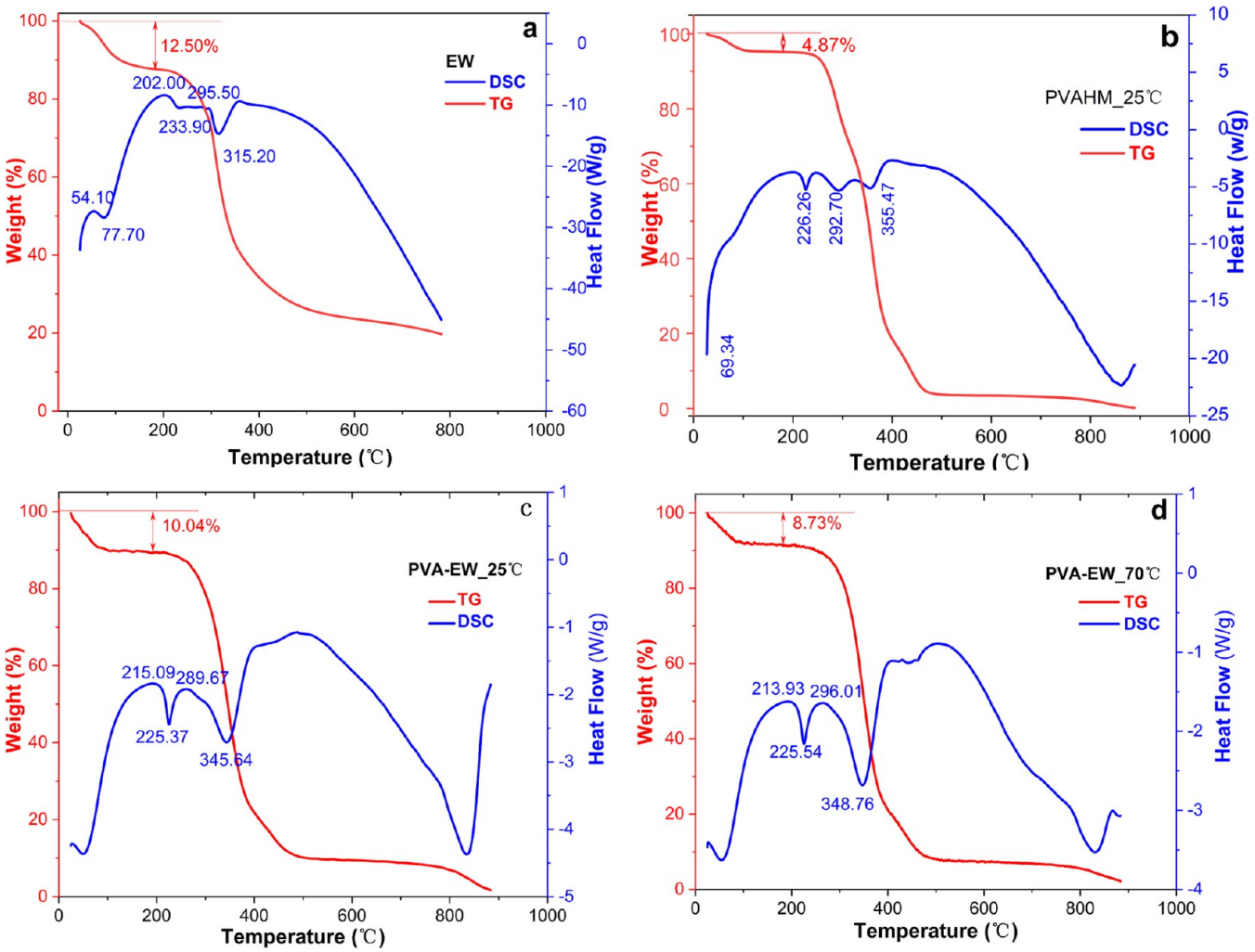


**Figure 6.** Effect of temperature during unidirectional dehydration on thermal properties of PVA−EW hydrogel composite membranes. TG and DSC of egg white (EW) powder (a), PVA hydrogel film without EW (PVAHM_25 °C) at 25 °C (b), and PVA−EW (20%) hydrogel composite membranes formed by UND at 25 and 70 °C (c, d).

hydrogen bonds. This is consistent with the significantly improved tensile properties reported in previous sections.

**3.8. SAXS Patterns.** The small-angle X-ray scattering (SAXS) patterns of PVA−EW hydrogel films formed by unidirectional dehydration at 25 and 70 °C were analyzed. Figure 5c shows the scattering intensity−scattering vector ($q$) curves of the PVA−EW (20%) hydrogel composite film obtained using SAXS. The figure shows that the two hydrogel membranes have very clear scattering peaks, while the evaporation membranes (PVA−EW_EA) prepared by slow evaporating and drying using the casting method do not exhibit scattering peaks. This shows that unidirectional dehydration through nanopores promotes the formation of ordered structures in the PVA−EW hydrogel composite film. The crystalline form of the hydrogel film is exhibited as lamellae, and the scattering peaks are caused by the scattering interference between the lamellae. The long period represents the statistical average distance between the lamellae and can be calculated using Bragg's law ($2\pi/Q$). The intercrystallite spacings ($d$) of the PVA−EW hydrogel membranes formed at 25 and 70 °C are 12.92 and 12.84 nm, respectively, indicating that there is almost no change in the intercrystallite spacing between these two temperature regimes. This shows that the significant difference between the intensity of the scattering peaks between the two samples is not dependent on the spacing $d$ between the lamellae. When unidirectional dehydration is carried out at 70 °C, the molecular motion is accelerated, the film-forming time is significantly shortened, and the thickness of the formed hydrogel film is thinner than those formed at 25 °C. In addition, strong hydrogen bonds are formed between the molecules, resulting in a denser structure and enhanced mechanical properties, especially with regard to tensile strength. However, due to the rapid dehydration, the regularity of the thickness and spacing of the lamellae decreases, causing the intensity of the scattering peak to be significantly reduced to half the value observed at 25 °C. These results suggest that the temperature of UND has a significant effect on the regularity of the lamella structure in PVA−EW hydrogel composite films.

**3.9. Thermal Analysis.** Figure 6 presents the thermal analytical TG and DSC patterns of the PVA−EW hydrogel composite films produced under two different processing temperatures. It also presents the patterns of pure EW powder and pure PVA hydrogel film (PVAHM) as two experimental controls. First, it should be noted that the water content of the pure EW powder is as high as 12.50%. The water evaporates after it reaches 202.00 °C, at which point it absorbs more heat and reaches the glass-point-transition temperature at 233.90 °C, and reaches a peak thermal decomposition temperature at 315.20 °C



https://doi.org/10.1021/acsomega.3c04171
ACS Omega 2023, 8, 33763−33773

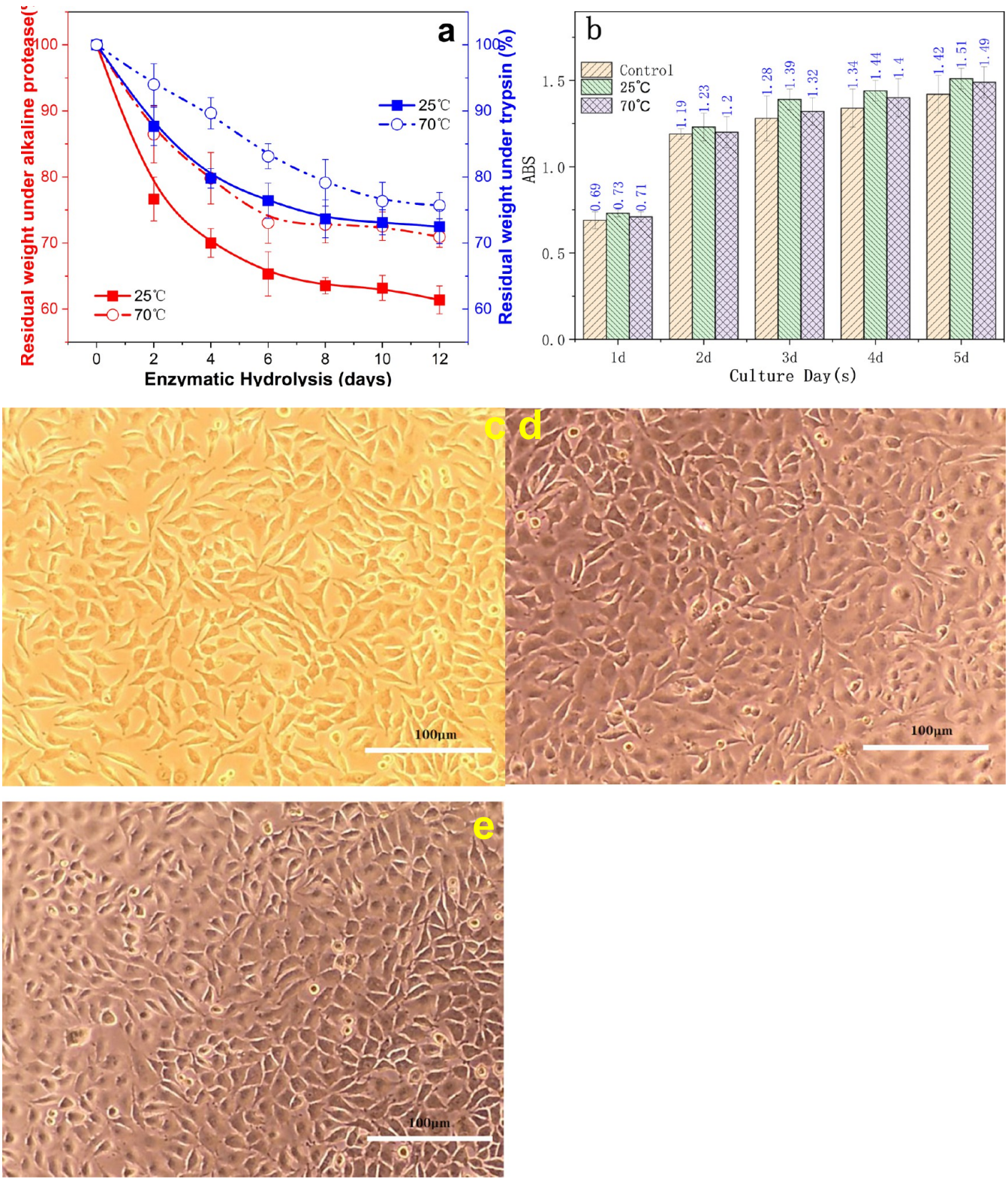


**Figure 7.** Protease resistance of the two PVA−EWs and their biocompatibility. Influence of temperature on of two UND-based PVA−EWs(20%) at 25 and 70 °C to both trypsin and alkaline protease (a), 5-day growth histograms of L-929 cells on the two hydrogel membrane and control (b), control group without film (c), and two UND-based PVA−EW (20%) hydrogel membranes at 25 and 70 °C (d, e).

(Figure 6a). In contrast, the water content of the pure PVA hydrogel film is only 4.87%. After heat absorption, the water reaches the glass-point temperature at 226.26 °C, after which there are two thermal decomposition temperature peaks at 292.70 °C and 355.47 °C. This is likely due to the weak and strong hydrogen bonds formed in the hydrogel membrane due to UND (Figure 6b). After the addition of 20% EW, the water content of the composite hydrogel film formed at 25 °C increased significantly to 10.04%. Furthermore, the glass-point-transition temperature after the endotherm was 225.37 °C and



https://doi.org/10.1021/acsomega.3c04171
ACS Omega 2023, 8, 33763−33773

the first thermal degradation peak disappeared, while the second degradation peak moved forward significantly, appearing at 345.64 °C. This indicates that the thermal stability of the mixed PVA−EW composite film was reduced (Figure 6c). However, when the temperature of the UND process was raised to 70 °C, the water content of the hydrogel film reduced, and the thermal decomposition temperature significantly increased to 348.76 °C (Figure 5d); this result is consistent with the enhanced stretching observed in previous experiments. These results show that increasing the UND temperature allows for the formation of either more hydrogen bonds or stronger hydrogen bonds between the hydroxyl groups in the PVA chain and the hydroxyl groups of EW protein. The thermal stability of the hydrogel composite film at 70 °C is significantly higher than the hydrogel film prepared at 25 °C; this shows that the thermal stability of the hydrogel composite membrane can be controlled by the temperature of the process.

**3.10. Antiprotease Ability.** To assess the resistance of the PVA−EW hydrogel composite membrane to proteases, an in vitro enzymolysis test with two proteases was performed. The values presented in Figure 7a are the residual amounts (recorded every 2 days) of PVA−EW (20%) hydrogel membranes that were enzymatically hydrolyzed. The figure shows that the residual amounts of the hydrogel membranes in the two protease aqueous solutions decrease over several days of enzymatic hydrolysis. As the number of hydrolyzed days prolonged and decreased, the overall enzymatic hydrolysis trend was similar. 79.80 and 89.67% of the two hydrogel membranes (PVA−EW (20%) _25 and _70 °C) remained in the trypsin solution after 4 days, and only 72.47 and 75.67% were left on the 12th day. In the alkaline protease solution, the enzymatic hydrolysis of the two PVA−EW hydrogel membranes was much more rapid, leaving only 61.37 and 70.93% of the hydrogel membranes after 12 days. These results show that the degradation rate of the hydrogel film in the two enzymes was related to the temperature of the preparation process. The higher the temperature during the preparation of the PVA−EW hydrogel film, the slower the degradation rate in trypsin and alkaline protease. In addition, the rate of degradation of the hydrogel membranes by enzymatic hydrolysis was faster in alkaline protease than in trypsin. The PVA−EW hydrogel composite membrane formed by directional dehydration at higher temperatures has better resistance to enzymatic hydrolysis than membranes formed at lower temperatures. These results are consistent with those regarding the film's mechanical properties. These results thus indicate that temperature during UND can be used to adjust the resistance of the PVA−EW hydrogel composite membrane to enzymatic hydrolysis.

**3.11. Biocompatibility.** Figure 7b−e shows the growth and proliferation of mouse fibroblast L-929 on two PVA−EW hydrogel composite membranes over 5 days. In this experiment, a CCK-8 detection method was used to determine the viability of both the hydrogel membrane and a control group for 1−5 days. One day after the cells were seeded on the surface of the hydrogel, most of them were round, sparse, and evenly distributed on the surface of the bioscaffold. These cells gradually adhered and attached themselves to the bioscaffold, and changed from a spherical shape to a spindle shape. On the 4th day, the cells had proliferated across the surface of the hydrogel, were densely distributed on the surface of the bioscaffold, and almost all of them exhibited a spindle-like shape. The pseudopodia of the cells were stretched, took the form of a mature spindle shape, and the cells grew vigorously. After the first and second days, the two experimental groups and the control group had similar rates of cell growth, and their $ABS_{450}$ values were not significantly different. On the second day, the cells in all groups began to proliferate rapidly. Although the difference between the $ABS_{450}$ of the experimental groups and the control group was still relatively small, the experimental groups exhibited values that were slightly higher than the control group. On the fourth day, the optical density values of both the control and the two experimental groups were almost double that observed after the first day of growth. In addition, it was found that the cells grew and divided rapidly on the second day, but the rate of growth decreased after the third day. An analysis of the overall status of the cell growth showed that the growth of the cells in the control group was relatively flat and slender, while the cells in the two sample groups grew normally; specifically, the cells were comb-shaped, grew well, were relatively full, had a strong three-dimensional (3D) effect, and were of a higher density. They can almost be observed after zooming in. In the context of the cell's nucleus, the difference in production status between the two experimental groups prepared at 25 and 70 °C was not significant (Figure 7d,e). This may be because the basement membrane is a porous hydrogel composed of PVA and EW protein with good biocompatibility, allowing the two heads of the cell to stretch down and grow. This indicates that the PVA−EW hydrogel composite membrane is suitable for the adhesion, growth, and proliferation of L-929 cells. Thus, the PVA−EW hydrogel composite membrane has excellent porosity and biocompatibility, and can be used as a potential substrate for cell cultures.

## 4. DISCUSSION

Pure EWs can also be made into a hydrogel, but the resulting hydrogel film can dissolve in water. EW hydrogels can be prepared by boiling EWs at 98 °C for 15 min and then placing them into a refrigerator at 5 °C and 60% RH for 2 weeks. After dehydration, the material becomes hard and is somewhat similar to plastic, but no further investigation has been made regarding the resultant material's characteristics, mechanical and physicochemical properties, and its stability in water.[41] Someone also investigated EW bioplastics produced by the addition of glycerin via a thermomechanical processing method.[42] Just recently, the author has also developed a green three-step processing method involving a "steaming-slow drying-annealing" process to prepare pure EW hydrogel films. This film is soft, translucent, and has strong mechanical and swelling properties;[33] it has the potential to be used in the development of materials for medical tissue engineering. However, in all of the technologies described, high-temperature heat treatment is still required to denature the EW protein to form a water-insoluble hydrogel material.

In addition, an oriented porous biological material can be obtained from an aqueous PVA solution via directional freezing and room-temperature thawing. This material has significantly improved mechanical properties and is more suitable for the implantation of medical stents such as anisotropic organs.[43−45] However, the preparation process of these anisotropic PVA hydrogels or composite hydrogel materials requires extremely low-temperature processing and room-temperature circulation. Furthermore, the processing process is difficult to control, and it is difficult to add living cells to these scaffolds.

In this experiment, a green and environmentally friendly hydrogel composite material was produced by combining EW, which exhibits poor mechanical properties, and PVA. The process does not require any physical or chemical treatment at


https://doi.org/10.1021/acsomega.3c04171
ACS Omega 2023, 8, 33763−33773

room temperature and can only be dehydrated using a nanopore semipermeable cellulose membrane. The PVA−EW hydrogel composite membrane produced has strong mechanical properties. During processing, the physical, chemical, and mechanical properties of the PVA−EW hydrogel composite membrane can be controlled by the amount of EW used and the processing temperature. This is highly desirable to tailor the material to various applications such as biomaterials and biomedicine, especially in the form of artificial skin, implants in the body, wound dressings, etc.

## 5. CONCLUSIONS

After incorporating 20% EW, a PVA−EW hydrogel obtained by UND at 25 °C still possesses a tensile strength of 0.91 MPa, an elongation at break of 534.17%, and a swelling rate of 230%. As the temperature during UND increases between 25 and 70 °C, the resulting PVA−EW improves in mechanical properties and thermal stability. The tensile strength of UND-based PVA−EW at 70 °C was seven times stronger than the hydrogel produced at 25 °C, and the elongation at break increased to 738.86%. UND results in the ordered rearrangement of PVA molecules and EW protein molecules, which increases or strengthens the hydrogen bonds that form in PVA intramolecular and intermolecular chains. PVA−EW had an ordered lamellar structure with a pore size between 1 and 10 $\mu$m. The residual amount of PVA−EW hydrogel after in vitro trypsin hydrolysis for 12 days is greater than the amount that remained after in vitro alkaline protease hydrolysis. Mouse fibroblast L-929 was found to be able to adhere, grow, and proliferate well on a PVA−EW bioscaffold. The experimental results show that the mechanical properties of the composite hydrogel membrane can be controlled by EW content and unidirectional nanopore dehydration temperature. The PVA−EW composite hydrogel membrane has potential development values and application in the fields of biomaterials, artificial skin, beauty facial mask, bionic materials, medical tissue engineering materials, etc.

## AUTHOR INFORMATION

### Corresponding Authors

**Ji-Xin Li** − *School of Biology and Basic Medical Sciences, Medical College, Soochow University, Suzhou 215123, P. R. China*; Email: 20205221002@stu.suda.edu.cn

**Yu-Qing Zhang** − *School of Biology and Basic Medical Sciences, Medical College, Soochow University, Suzhou 215123, P. R. China*; orcid.org/0000-0001-7670-386X; Email: sericult@suda.edu.cn

Complete contact information is available at: https://pubs.acs.org/10.1021/acsomega.3c04171

### Notes

The authors declare no competing financial interest.

## ACKNOWLEDGMENTS

This study was funded by the China Agriculture Research System (CARS-18-ZJ0502) and the Priority Academic Program Development of Jiangsu Higher Education Institutions (PAPD).

## REFERENCES

(1) Bakhsheshi-Rad, H. R.; Ismail, A. F.; Aziz, M.; et al. Development of the PVA/CS Nanofibers Containing Silk Protein Sericin as a Wound Dressing: In Vitro and in Vivo Assessment. *Int. J. Biol. Macromol.* **2020**, *149*, 513−521.

(2) Sapalidis, A. A.; Katsaros, F. K.; Romanos, G. E.; et al. Preparation and Characterization of Novel Poly-(Vinyl Alcohol)−Zostera Flakes Composites for Packaging Applications. *Composites, Part B* **2007**, *38*, 398−404.

(3) Amanda, A.; Kulprathipanja, A.; Toennesen, M.; et al. Semi-crystalline Poly (Vinyl Alcohol) Ultrafiltration Membranes for Bioseparations. *J. Membr. Sci.* **2000**, *176*, 87−95.

(4) Dong, Y.; Zhang, Y.; Tu, B. Immobilization of Ammonia-Oxidizing Bacteria by Polyvinyl Alcohol and Sodium Alginate. *Braz. J. Microbiol.* **2017**, *48*, 515−521.

(5) Figueiredo, K. C. S.; Alves, T. L. M.; Borges, C. P. Poly (vinyl alcohol) Films Crosslinked by Glutaraldehyde Under Mild Conditions. *J. Appl. Polym. Sci.* **2008**, *111*, 3074−3080.

(6) Han, B.; Li, J.; Chen, C.; et al. Effects of Degree of Formaldehyde Acetal Treatment and Maleic Acid Crosslinking on Solubility and Diffusivity of Water in PVA Membranes. *Chem. Eng. Res. Des.* **2003**, *81*, 1385−1392.

(7) Li, R. H.; Barbari, T. A. Protein Transport through Membranes Based on Toluene Diisocyanate Surface-Modified Poly (Vinyl Alcohol) Gels. *J. Membr. Sci.* **1994**, *88*, 115−125.

(8) Nishiyabu, R.; Kobayashi, H.; Kubo, Y. Dansyl-Containing Boronate Hydrogel Film as Fluorescent Chemosensor of Copper Ions in Water. *RSC Adv.* **2012**, *2*, 6555−6561.

(9) Ali, A.; Nouseen, S.; Saroj, S.; et al. Repurposing Pinacol Esters of Boronic Acids for Tuning Viscoelastic Properties of Glucose-Responsive Polymer Hydrogels: Effects on Insulin Release Kinetics. *J. Mater. Chem. B* **2022**, *10*, 7591−7599.

(10) Ali, A.; Saroj, S.; Saha, S.; Rakshit, T.; Pal, S. In Situ-Forming Protein-Polymer Hydrogel for Glucose-Responsive Insulin Release. *ACS Appl. Bio Mater.* **2023**, *6*, 745−753.

(11) Sirousazar, M.; Khadivi, H. Delir S. Swelling and Drying Mechanisms of Freeze-Thawed Polyvinyl Alcohol/Egg White/Montmorillonite Bionanocomposite Hydrogels. *J. Macromol. Sci., Part B* **2020**, *59*, 309−330.

(12) Eghbalifam, N.; Frounchi, M.; Dadbin, S. Antibacterial Silver Nanoparticles in Polyvinyl Alcohol/Sodium Alginate Blend Produced by Gamma Irradiation. *Int. J. Biol. Macromol.* **2015**, *80*, 170−176.

(13) Bolto, B.; Tran, T.; Hoang, M.; et al. Crosslinked Poly (Vinyl Alcohol) Membranes. *Prog. Polym. Sci.* **2009**, *34*, 969−981.

(14) Oviedo, I. R.; Mendez, N. A. N.; Gomez, M. P. G.; et al. Design of a Physical and Nontoxic Crosslinked Poly (Vinyl Alcohol) Hydrogel. *Int. J. Polym. Mater.* **2008**, *57*, 1095−1103.

(15) Patil, S.; Bharimalla, A. K.; Mahapatra, A.; et al. Effect of Polymer Blending on Mechanical and Barrier Properties of Starch-Polyvinyl Alcohol Based Biodegradable Composite Films. *Food Biosci.* **2021**, *44*, No. 101352.

(16) Moreira, B. R.; Pereira-Júnior, M. A.; Fernandes, K. F.; et al. An Ecofriendly Edible Coating Using Cashew Gum Polysaccharide and Polyvinyl Alcohol. *Food Biosci.* **2020**, *37*, No. 100722.

(17) Wang, R.; Li, N.; Jiang, B.; et al. Facile Preparation of Agar/Polyvinyl Alcohol-Based Triple-Network Composite Hydrogels with Excellent Mechanical Performances. *Colloids Surf., A* **2021**, *615*, No. 126270.

(18) Bai, M.-Y.; Hsueh, Y-W. Evaluation of silk fibroin protein/poly (vinyl alcohol) transparent membranes as prospective patch for acne care. *J. Bioact. Compat. Polym.* **2015**, *30*, 490−508.

(19) Su, J. F.; Huang, Z.; Zhao, Y. H.; et al. Moisture Sorption and Water Vapor Permeability of Soy Protein Isolate/Poly (Vinyl Alcohol)/Glycerol Blend Films. *Ind. Crops Prod.* **2010**, *31*, 266−276.

(20) Durmaz, B. U.; Aytac, A. Development and characterization of poly (vinyl alcohol) and casein blend films. *Polym. Int.* **2019**, *68*, 1140−1145.

(21) Durmaz, B. U.; Aytac, A. Development and Characterization of Poly (Vinyl Alcohol) and Casein Blend Films. *Polym. Int.* **2019**, *68*, 1140−1145.

(22) Biranje, S.; Madiwale, P.; Adivarekar, R. V. Porous Electrospun Casein/PVA Nanofibrous Mat for Its Potential Application as Wound Dressing Material. *J. Porous Mater.* **2018**, *26*, 29−40.

(23) Xie, J.; Hsieh, Y-L. Ultra-High Surface Fibrous Membranes from Electrospinning of Natural Proteins: Casein and Lipase Enzyme. *J. Mater. Sci.* **2003**, *38*, 2125−2133.
(24) Pranata, M. P.; González-buesa, J.; Chopra, S.; Kim, K.; Pietri, Y. Egg white protein film production through extrusion and calendering processes and its suitability for food packaging applications. *Food Bioprocess Technol.* **2019**, *12*, 714−727.
(25) Yaping, H. E.; Hang, D. Z.; Ong, S. D.; Heng, J. Z. A novel nitrite biosensor based on gold dendrites with egg white as template. *Anal. Sci.* **2012**, *28*, 403−409.
(26) Hu, G.; Batool, Z.; Cai, Z.; et al. Production of Self-Assembling Acylated Ovalbumin Nanogels as Stable Delivery Vehicles for Curcumin. *Food Chem.* **2021**, *355*, No. 129635.
(27) Shojaee, M.; Navaee, F.; Jalili-Firoozinezhad, S.; et al. Fabrication and Characterization of Ovalbumin Films for Wound Dressing Applications. *Mater. Sci. Eng.: C* **2015**, *48*, 158−164.
(28) López-Mata, M. A.; García-González, G.; Valbuena-Gregorio, E.; et al. Development and Characteristics of Biodegradable Aloe-Gel/Egg White Films. *J. Appl. Polym. Sci.* **2016**, *133*, No. 44067.
(29) Shaabani, Y.; Sirousazar, M.; Kheiri, F. Synthetic−Natural Bionanocomposite Hydrogels on the Basis of Polyvinyl Alcohol and Egg White. *J. Macromol. Sci., Part B* **2016**, *55*, 849−865.
(30) Kumar, A.; Negi, Y. S.; Choudhary, V.; et al. Effect of Modified Cellulose Nanocrystals on Microstructural and Mechanical Properties of Polyvinyl Alcohol/Ovalbumin Biocomposite Scaffolds. *Mater. Lett.* **2014**, *129*, 61−64.
(31) Zhang, X.; Zou, W.; Xia, M.; et al. Intelligent Colorimetric Film Incorporated with Anthocyanins-Loaded Ovalbumin-Propylene Glycol Alginate Nanocomplexes as a Stable PH Indicator of Monitoring Pork Freshness. *Food Chem.* **2022**, *368*, No. 130825.
(32) Mani, M. P.; Jaganathan, S. K. Blood compatibility assessments of novel electrospun PVA/egg white nanocomposite membrane. *Bio-inspired, Biomimetic Nanobiomater.* **2016**, *7*, 213−218.
(33) Lu, T.; Zou, Q.; Zhu, K.; et al. Electrospun Egg White/Polyvinyl Alcohol Fiber Dressing to Accelerate Wound Healing. *J. Polym. Res.* **2021**, *28*, No. 67.
(34) Zhang, M.; Zhang, Y-Q.; Wang, H.-Y. Unidirectional nanopore dehydration induces to form highly stretchable and mechanically robust silk fibroin membranes dominated by type II beta-turns. *ACS Biomater. Sci. Eng.* **2023**, *9*, 2741−2754.
(35) Jing, F.-Y.; Zhang, Y-Q. Unidirectional Nanopore Dehydration Induces an Anisotropic Polyvinyl Alcohol Hydrogel Membrane with Enhanced Mechanical Properties. *Gels* **2022**, *8*, No. 803.
(36) Wei, Z.-Z.; Dong, X.; Zhang, Y.-Q. A mechanically robust egg white hydrogel scaffold with excellent biocompatibility by three-step green processing. *Sci. China Technol. Sci.* **2022**, *65*, 1599−1612.
(37) Li, H. P.; Sui, J. X.; Zhang, X.; Wei, J. C.; Zhang, Y. M.; Bao-Lin. Optimization for hydrolyzing conditions of bioactive peptide from chicken albumen with neutral protease. *J. Food Sci. Technol.* **2009**, *34*, 186−189.
(38) Wang, H.-Y.; Zhang, Y.-Q.; Wei, Z-G. Characterization of Undegraded and Degraded Silk Fibroin and Its Significant Impact on the Properties of the Resulting Silk Biomaterials. *Int. J. Biol. Macromol.* **2021**, *176*, 578−588.
(39) Honda, A.; Huroda, N. Functional improvement in dried egg white through the Maillard reaction. *J. Agric. Food Chem.* **1999**, *47*, 1845−1850.
(40) Tan, J.; Liu, T.; Yao, Y.; Wu, N.; Tu, Y. Changes in physicochemical and antioxidant properties of egg white during the Maillard reaction induced by alkali. *LWT* **2021**, *12*, No. 111151.
(41) Nakamura, A.; Hara, K.; Hiramatsu, N.; et al. Low Frequency Raman Peak and Elastic Anomaly of Dehydrated Heat-Treated Egg-White Gel. *J. Phys. B* **1999**, *263*−*264*, 327−329.
(42) Jerez, A.; Partal, P.; Marti′nez, I.; Gallegos, C.; Guerrero, A. Egg white-based bioplastics developed by thermomechanical processing. *J. Food Eng.* **2007**, *82*, 608−617.
(43) Millon, L. E.; Mohammadi, H.; Wan, W. K. Anisotropic Polyvinyl Alcohol Hydrogel for Cardiovascular Applications. *J. Biomed. Mater. Res., Part B* **2006**, *79B*, 305−311.
(44) Zhang, H.; Cooper, A. Aligned Porous Structures by Directional Freezing. *Adv. Mater.* **2007**, *19*, 1529−1533.
(45) Zhang, L.; Zhao, J.; Zhu, J.; et al. Anisotropic Tough Poly (Vinyl Alcohol) Hydrogels. *Soft Matter* **2012**, *8*, 10439−10447.


https://doi.org/10.1021/acsomega.3c04171
*ACS Omega* 2023, 8, 33763−33773